Scientia Iranica B (2022) 29(5), 2279–2289

Sharif University of Technology
Scientia Iranica
Transactions B: Mechanical Engineering
http://scientiairanica.sharif.edu

A new micro pump for rapid and accurate microscale droplet manipulation using thermo-viscous actuation

M. Mehrabi[a] and A.H. Meghdadi Isfahani[a,b,*]

a. *Department of Mechanical Engineering, Najafabad Branch, Islamic Azad University, Najafabad, Iran.*
b. *Aerospace and Energy Conversion Research Center, Najafabad Branch, Islamic Azad University, Najafabad, Iran.*

Received 8 February 2021; received in revised form 24 September 2021; accepted 25 April 2022

KEYWORDS
Lab on a chip;
Droplet;
Thermo-viscose expansion;
Two-phase flow;
Bio;
Biofluidics

Abstract. Current study proposes a novel mechanism for micro-scale droplet generation. To this end, a new micro pump consisting of an expansion chamber with two nozzles on its left and right sides is introduced, which is capable of creating a unidirectional flow. In the current study, for the first time, thermo-viscose expansion method is used to actuate the flow by assuming that the fluid is heated using a laser beam source, leading to expansion and movement of the fluid. Two-phase flow analysis using the Volume Of Fraction (VOF) method shows that the proposed micro pump can consistently generate droplets with uniform and micro-scale dimensions.

1. Introduction

Microscale droplet generators have a wide range of applications in various industries including inkjet printers [1], microfluidic slug flow systems [2], and lab-on-a-chip setups [3,4]. Microfluid droplet generators offer much higher precision and repeatability than conventional microscale batch processes for continuous production of highly monodispersed emulsions. By tuning the relative viscosities, surface tensions, and velocities between dispersed and continuous phases, it is possible to create droplets with almost equal size.

The physical properties of micro-scale flows are different from those of macro-scale ones [5]. For micro- and nano-scale flows, the higher surface-to-volume ratio causes better heat transfer [6] than macro-scale flows. On the other hand, high surface-to-volume ratio indicates that the skin friction forces between fluid and walls and consequently, surface tensions are significant compared to body forces (fluid inertia) [7]. Therefore, in recent years, many studies have investigated flow control on micro and nano scales. Flow control at these dimensions is always challenging and existing methods are unable to meet some of the needs of the researchers.

In droplet generation processes, continuous generation of small droplets with constant distances and constant generation speeds is essential [8]. Therefore, droplet generation and movement processes and control methods for droplet diameters are of high significance [9].

The first study investigating droplet generation and formation using continuous jet flows was carried out by Lord Riley [10] which was the base of inkjet printers.

Droplet generation methods can be divided into passive and active methods:

1. **Passive methods (hydrodynamic methods)**, including T-junction, Cross-junction, and co-flowing methods, are the methods that do not require external power. The basis of these methods is the use of a shear strain mechanism, which is

*. *Corresponding author. Tel.: +983142292530*
E-mail address: amir_meghdadi@pmc.iaun.ac.ir (A.H. Meghdadi Isfahani)

doi: 10.24200/sci.2022.57704.5375

usually applied from one fluid to another based on their relative placement. In this regard, Kalantarifard et al. [11] demonstrated that reduction of hydrodynamic pressure loss in T-junctions improved monodispersity of droplets. Hoseinpour and Sarreshtehdari [12] demonstrated that in a T-shaped microchannel, for low capillary numbers, decreasing the junction angle from 90° to 80° and 60° causes smooth mixing of fluids for the reaction without any vibration or shaking. Teo et al. [13] demonstrated successful micro droplet manipulation in T-junctions by applying an AC electric field. In another study, Tan et al. [14] used a liquid-liquid mechanism in an orifice cross-section to produce micro-scale droplets. They managed to control droplet diameter by controlling input flow rates. In another study [15], the effect of using nanofluids on droplet formation in T-junction micro channels was investigated. It was concluded that using nanofluids decreased droplet size. Therefore, nanofluids can be used as good alternatives rather than chemical additives in droplet generation systems;

2. **Active methods** are methods that require external power. Some of the active methods are:
   - *Droplet generation using pneumatic actuators [16,17]* in which an air chamber (syringe) is used for actuating fluid and droplet generation;
   - *Droplet generation using piezoelectric actuators* in which a piezoelectric crystal is used for actuating the fluid and droplet generation [18]. For example, Li et al. [19] developed a resonant piezoelectric to generate continuous micro-droplets from high viscosity liquids. They mentioned that the silicone oil with the large viscosity of 150 cps could be easily manipulated by the proposed system;
   - *Droplet generation using optical actuation:* Using optical power to manipulate and control microscale droplets in liquid has attracted growing attention in the field of microfluidics [20]. In this method, cavitation bubbles are created in water by laser irradiation which pushes water into the oil to generate aqueous droplets [21]. On the other hand, the droplet size and generation frequency can be changed using this method because heating the fluid by optical techniques reduces the viscosity and interfacial tension, leading to changes in droplet diameter [22,23].

   Acoustic actuators, pneumatic actuators, electrostatic actuators, and electro-hydrodynamic actuators are other actuators used for active droplet generation [24].

In recent years, flow excitation and mixing of two flows using a focused light beam based on the thermo-viscose expansion method have been proposed [25]. In this method, a periodic temperature distribution is applied to the fluid via a light beam, which causes the fluid to be alternately heated and cooled. With increase in fluid temperature as a result of the light beam, the fluid expands and its viscosity decreases, which leads to the movement of the fluid. Viscosity variations versus temperature are shown in Figure 1.

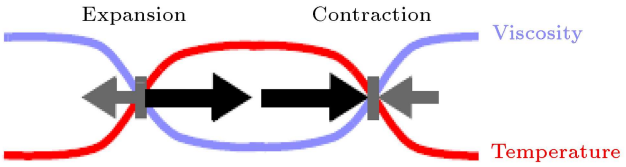

Figure 1. Viscosity changes with temperature.

Heating using a laser beam is important because it is able to create very small temperature oscillations within fast pulses in the fluid and, thus, to fully control fluid movements. According to the findings of Yariv and Brenner [26], even in the absence of gravity, unsteady temperature fields in thermally expandable fluids will always be accompanied by flow. Pal and Chakraborty [27] used this approach to investigate a generated time-averaged spatially uniform flow profile by imposing traveling temperature wave in a microfluidic channel. They found that flow rate was a linear function of Reynolds number. In another work, considering periodic temperature oscillation over a flat plate, Pal and Chakraborty [28] reported that the entire thermal fluctuation and the subsequent thermos-viscous actuation (for a semi-infinite fluid bounded by a flat plate) were confined within a thermo-viscous boundary layer. They proposed three different layers, namely the wall layer, the intermediate layer, and the outer layer, based on the length scales and the analytical solution for the temperature field, and demonstrated that a unidirectional time-averaged flow within the wall layer opposite to the direction of motion of the thermal wave occurred.

Furthermore, several studies on microscale flow generation and micro mixing by thermo viscous expansion due to laser spot movement were carried out by Weinert et al. [29–31].

As mentioned in the literature review, to this day, the thermo-viscose expansion method was used only for moving the fluid or mixing enhancement in the microchannels and no study has investigated droplet formation using this method. The aim of this study is the simulation and feasibility study of micro-scale droplet generation using thermo-viscose expansion. To this end, a new geometry is proposed for droplet-generating microchannel and a new function is introduced for temperature distribution using a laser beam.

2. Governing equations

In the current study, the Volume Of Fraction (VOF) model is used which is designed for following the location of free surfaces of two or more immiscible fluids [32]. The success of this method for simulation of flows and droplet deformations has been demonstrated in previous studies [33].

The governing equations are continuity, momentum, and energy equations. When two fluids are in contact with each other, mass transfer equation is also added to these equations.

The general form of continuity equation is as follows:

$$\frac{D\rho}{Dt} + \vec{\nabla} \cdot \rho\vec{V} = 0. \tag{1}$$

The changes in density and viscosity of two phases in their cross-section are presented by Eqs. (2)–(7) [34]:

$$\rho(x,t) = \rho_g + (\rho_l - \rho_g)\alpha(x,t), \tag{2}$$

$$\rho_l = \rho_{l0}[1 - \alpha_T(T - T_0)], \tag{3}$$

$$\rho_g = cte, \tag{4}$$

$$\mu(x,t) = \mu_g + (\mu_l - \mu_g)\alpha(x,t), \tag{5}$$

$$\mu_l = \mu_{l0}[1 - \eta_T(T - T_0)], \tag{6}$$

$$\mu_g = cte, \tag{7}$$

where ρ_0 and μ_0 are density and viscosity at the reference temperature, T_0. Given the fact that in the current study, only water is considered in thermo-viscose expansion, Eqs. (5) and (6) are suggested in which α_T is the thermal expansion coefficient that shows the volume changes in the fluid over time based on the reference temperature, while η_T is the thermal viscosity coefficient. T is the temperature of each cell that changes over time. α is the ratio of volume of each phase to the volume of the cell, which is defined using the following conditions in VOF method:

$$\begin{cases} \alpha = 1 & \text{water} \\ 0 < \alpha < 1 & \text{water-air interface} \\ \alpha = 0 & \text{air} \end{cases} \tag{8}$$

The value of α is determined through the phase transfer equation [35]:

$$\frac{D\alpha}{Dt} = \frac{\partial\alpha}{\partial t} + \vec{V} \cdot \Delta\alpha = 0. \tag{9}$$

The momentum equation for incompressible flows is:

$$\frac{\partial}{\partial t}\left(\rho\vec{V}\right) + \nabla, \left(\rho\vec{V}\vec{V}\right) = -\nabla P + \left[\mu\left(\nabla\vec{V} + \nabla^2\vec{V}\right)\right] + F_s. \tag{10}$$

The surface tension model used in this study is the Continuum Surface Force (CSF) model. In this model, the forces resulting from surface tension are calculated using the following equation:

$$F_s = \sigma\kappa\nabla\alpha. \tag{11}$$

Interface curvature is calculated using the following equation [35]:

$$\kappa = \nabla \cdot \left(\frac{\nabla, \alpha}{|\nabla, \alpha|}\right). \tag{12}$$

Furthermore, energy equation is:

$$\rho C_p \frac{DT}{Dt} = \alpha_T T \frac{DP}{Dt} + \vec{\nabla} \cdot \left(k\vec{\nabla}T\right). \tag{13}$$

By substituting Eq. (13) in continuum and density equations, the following equation is produced:

$$-\rho_0\alpha_T\frac{DT}{Dt} + \rho_0[1 - \alpha_T(T - T_0)]\vec{\nabla} \cdot \vec{V} = 0. \tag{14}$$

The properties of fluids used in the current study (water and air) are shown in Table 1.

Table 1. Properties of fluids used in this study.

Parameter	Value (unit)
ρ_{l0}	998.2 (kg/m^3)
ρ_g	1.225 (kg/m^3)
μ_{l0}	0.001003 (kg/m.s)
μ_g	1.7894×10^{-5} (kg/m.s)
α_T	3.0×10^{-4} (K^{-1})
η_T	2.2×10^{-2} (K^{-1})

3. Validation

3.1. Comparison with the results of Tan et al. [14]

Micro- and nano-scale droplet generation using piezoelectric actuators was investigated in an experimental study by Tan et al. [14]. The schematic of this mechanism is shown in Figure 2. The basis of this mechanism is controlling the mass flow of two fluids in which oil is used as the continuous phase, while water is

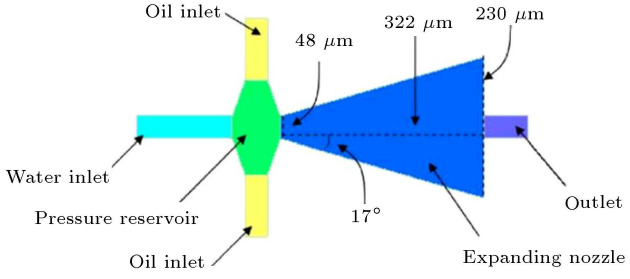

Figure 2. Schematic of the mechanism proposed by Tan et al. [14].

Figure 3. Formation of water droplets in oleic acid [14].

considered as the separated phase. Both water and oil fluids enter the cylindrical geometry shown in Figure 2 and droplets are formed on the surface of water due to shear strain derived from one of the fluids (oleic acid) and shape geometry. Figure 3 shows the formation of water droplets in oleic acid reported by Tan et al. [14]. Figures 4 and 5 show the results of the current study. Droplet shapes and radii are in good agreement with the experimental results of Tan et al. [14].

3.2. Comparison with the results of Winter et al. [29]

Winter et al. [29] investigated the microscale fluid flow induced by thermo-viscose expansion effects due to a traveling temperature wave. They used a Gaussian temperature distribution function ($\delta T(\vec{r}) = \delta T_0 \cos(kx) e^{\frac{-\gamma^2}{2b^2}}$) in order to heat and stimulate the fluid in which k is calculated using the wavelength equation $\lambda = \frac{2\pi}{k}$, b is the wave bandwidth, and δT_0 is the range of temperature oscillations. Figure 6 compares the fluid velocity obtained by Weinter et al. [29] with those of the present work. Figure 7(a) and (b) present the temperature wave induced in the fluid due to the laser beam obtained by Weinter et al. [29] and the present study, respectively. Good agreement between the results can be seen.

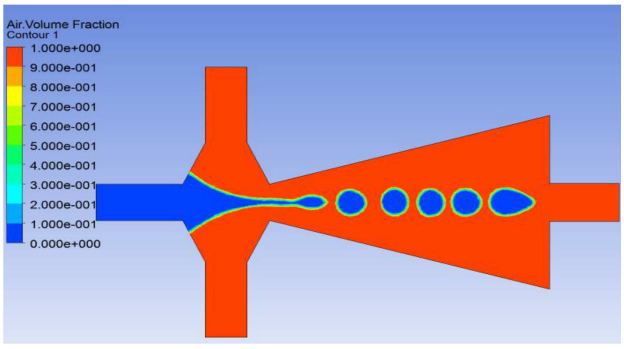

Figure 4. Formation of water droplets in oleic acid $Q_{\text{oil}} = 6$ µl/min and $Q_{\text{water}} = 0.5$ µl/min [14].

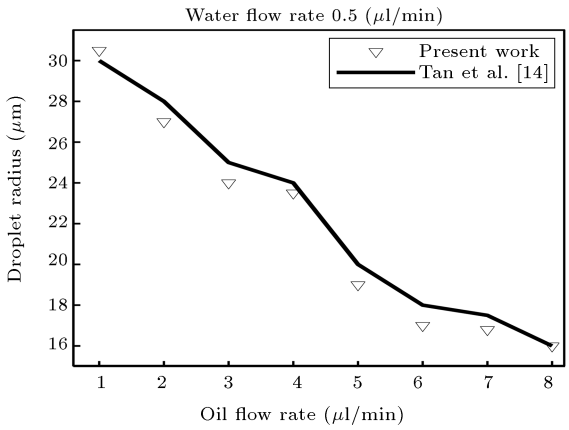

Figure 5. Droplet radius versus oil flow rate.

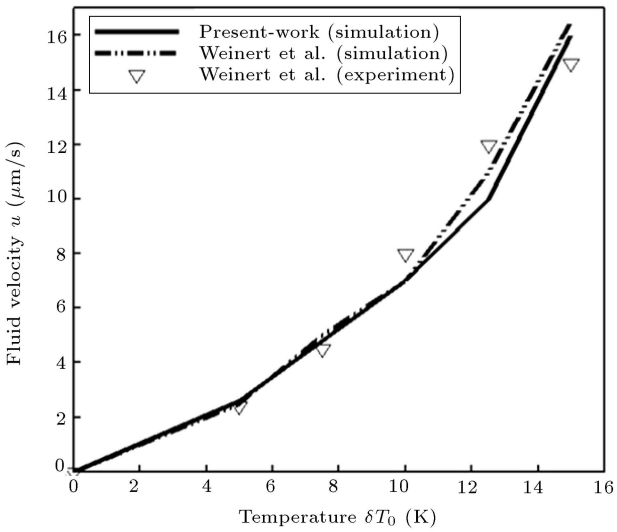

Figure 6. Effects of temperature change on flow velocity in the study by Weinert et al. [29].

4. Geometry of microchannel

The novel geometry used in the present paper to create micro droplets is shown in Figures 8 and 9. This method uses temperature oscillations produced using a laser beam to generate droplets. This geometry consists of two nozzles filled with water injected in the air flow in the right-hand channel. An expansion chamber is placed between these two nozzles in which water is heated and expanded using a laser beam. In this model, water is used as the separated fluid, while

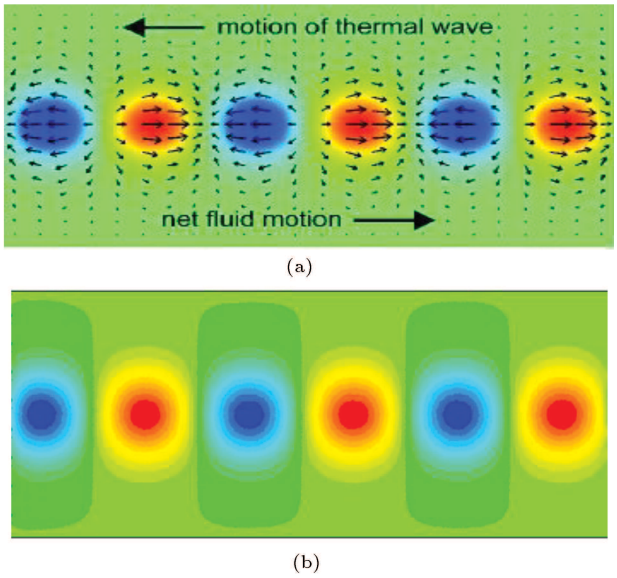

Figure 7. Temperature contours presented by (a) Weinert et al. [29] and (b) the present study.

air is used as the continuous fluid. The expansion chamber is characterized by 300 μm length and 200 μm width. Diameter of the nozzles changes depending on the geometry of the setup. However, the geometry of air injection channel is unchanged (length: 800 μm and width: 500 μm). The current study proposes the following Gaussian temperature distribution function for thermal actuation of the fluid:

$$T(x,y,t)=283+C\cos\left(\frac{\pi}{\lambda}x\right)e^{\frac{-y^2}{2b^2}}\left(1-\sin\left(\frac{t\pi}{180}\right)\right), \quad (15)$$

where $\lambda = 700$ μm is the wavelength and $b = 200$ μm is the bandwidth of the laser beam. According to Eq. (15), temperature alternately changes versus x and t. Heating causes an increase in the volume of water

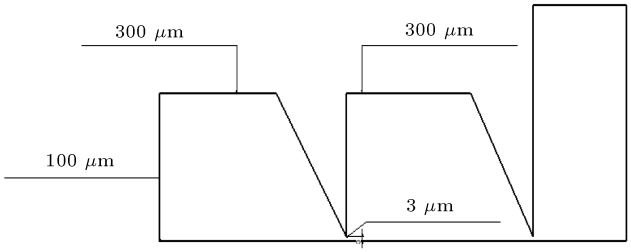

Figure 9. Technical characteristics of the proposed microchannel.

inside expansion chamber, causing the fluid to exit the tank. Since the diameter on the left side of the chamber is very small, water exits from the right side, which yields micro droplets. Then, due to altering nature of the temperature, the temperature in the expansion chamber decreases, causing the water to contract. This results in water being sucked in from the left side in order to compensate for the pressure drop. In the next step, the water is heated again and droplet generation process is repeated.

This process is simulated using the VOF method. In order to create initial equilibrium conditions between two fluids so that none of the two phases can diffuse into each other, the pressure in border conditions at the entrance and exit is equal to atmospheric pressure with the initial temperature being constant in the entire area and equal to 283 K.

5. Results and discussion

As mentioned before, one of the main novelties of the current approach is using two nozzles in tandem as rectifier. The reason is that using one single nozzle does not lead to suitable results. As mentioned in Figure 10, using a single nozzle causes air to be sucked into the

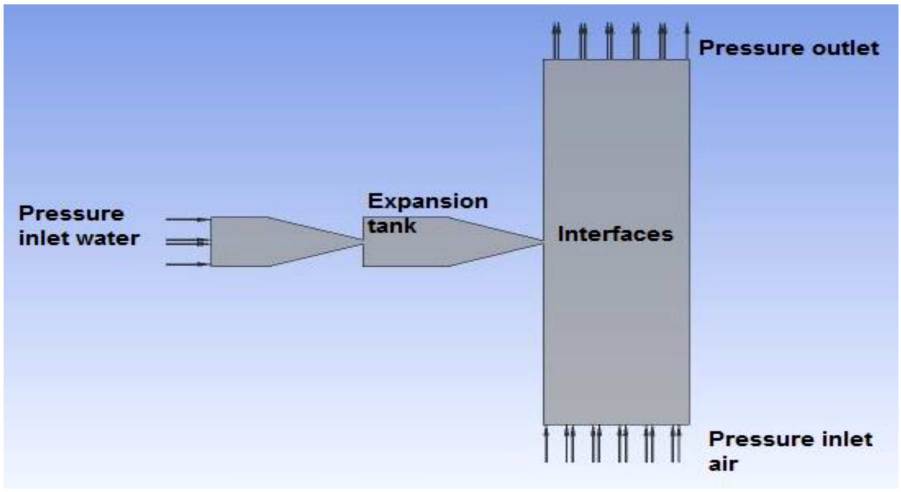

Figure 8. Schematic of the simulated microchannel with entrance and exit border conditions.

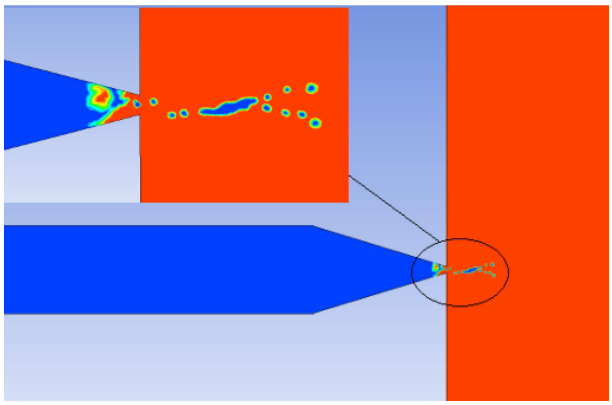

Figure 10. Schematic of the simulated microchannel with a single nozzle.

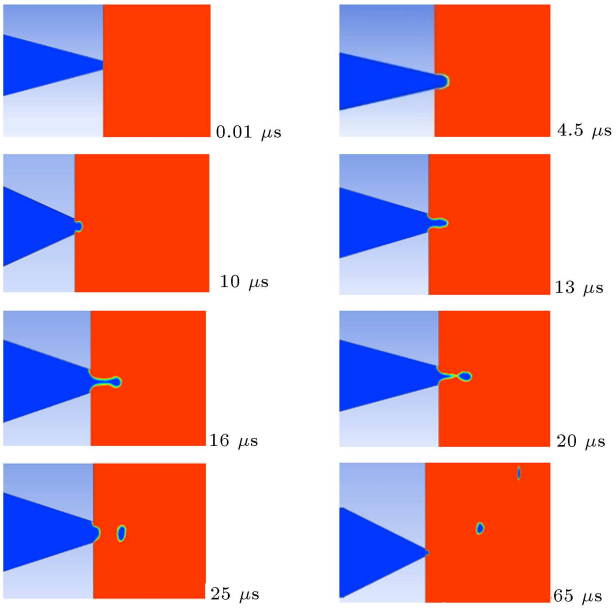

Figure 11. Droplet generation steps ($C = 0.5$).

nozzle, which means that the droplets will not have uniform diameters.

Figure 11 shows the effect of using two tandem nozzles on droplet generation by thermo-viscose expansion. In this setup, the only cause of flow in fluid film is the thermo-viscose expansion. Since fluid and flow properties are temperature dependent and temperature is applied to the fluid as a time-dependent heat wave, fluid flow acts similar to this wave. This means that we see the flow domain changes with a frequency equal to that of the heat wave.

In order to inject water into the air, it is necessary to have an actuator. As mentioned before, many previous studies use piezoelectric actuators for this purpose. In the present study, for the first time, thermo-viscose expansion is used for fluid actuation and droplet generation. To this end, the first fluid behavior was investigated without application of the Gaussian temperature function of Eq. (15). Pressure on both sides of nozzle was considered equal to atmospheric pressure and Navier–Stokes, continuum and energy equations were solved for both fluids at time steps of 0.01 microseconds to 1 second. The results demonstrated that two fluids were in equilibrium under these conditions.

After ensuring the initial equilibrium of fluids, water was actuated by using the Gaussian temperature of Eq. (15). Figure 11 shows the droplet generation process and water injection due to thermos-viscose expansion. By applying the heat function based on Eq. (15), water temperature increases locally, causing it to expand and move. Using a second nozzle on the left side of the main nozzle prevents flow to the left side. This means that the second nozzle creates a unidirectional flow. This causes the flow to move only to the right and generate droplets. Since water heats and cools in an alternating process, droplets form uniformly with similar diameters and at orderly time intervals.

Initially, the fluid volume starts to increase from 4.5 μs to 5 μs and begins contraction at 5 μs. Fluid reaches a semi-stable flow between 8 and 14.5 μs and thermal expansion starts again at 25 ms leading to the generation of the next droplet.

Since temperature changes directly affect thermo-viscose expansion, changes in parameters of Gaussian function (Eq. (15)) can control the volume and pressure of fluid exiting the nozzle, thus causing controlling droplet diameter. To this end, temperature, density, viscosity, and pressure were measured at the centerline of the expansion chamber (Figure 12, black line).

Figure 13 shows the viscosity variations along the centerline of the expansion chamber for various thermal wave amplitudes, C. This graph is a cosine graph and as expected, viscosity decreases with increase in temperature. Since, according to Eq. (15), the maximum temperature is at the center of the expansion chamber, this location will have the lowest viscosity. Decrease in viscosity decreases fluid friction with the walls and increases droplet diameter.

Figure 14 shows the density variations along the centerline of the expansion chamber for various thermal wave amplitudes. This graph is also a cosine graph in which density is reduced with increase in temperature. The decrease in density results from the expansion of the liquid due to heating, leading to droplet generation.

Figure 15 shows the effects of changes in output diameter of the nozzle on pressure distribution along the central line for $C = 0.5$ and $t = 50$ μs. Despite the symmetrical nature of temperature function (Eq. (15)) and density and viscosity distributions, pressure at the exit (right) of the expansion chamber is lower than that at the entrance (left) of the expansion chamber. The reason is using the second nozzle on the left side of the expansion chamber, which increases pressure and

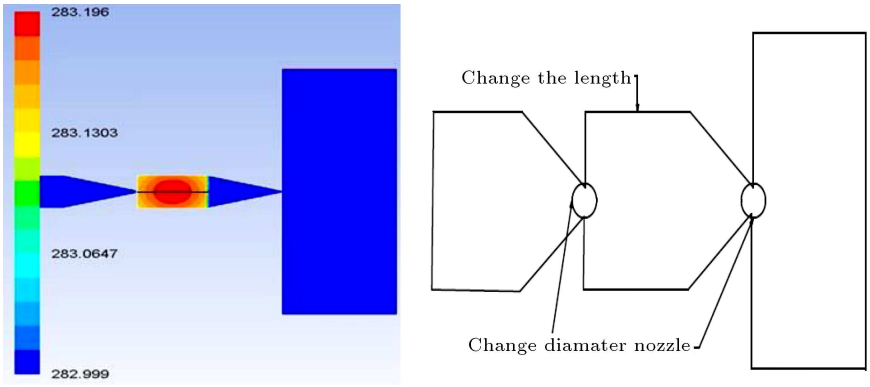

Figure 12. Temperature contour and measurement location for fluid properties.

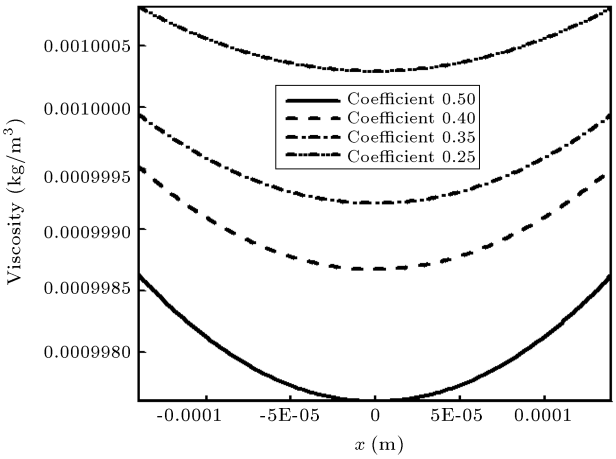

Figure 13. Viscosity variations along the centerline of the expansion chamber for various thermal wave amplitudes.

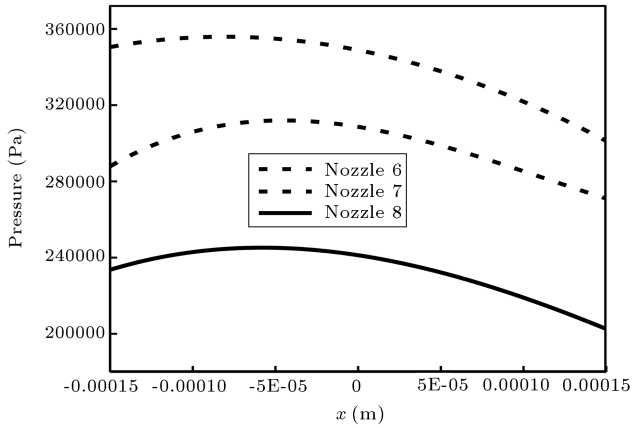

Figure 15. Pressure changes at the center of expansion chamber for thermal coefficient of 0.5 at 50 μs.

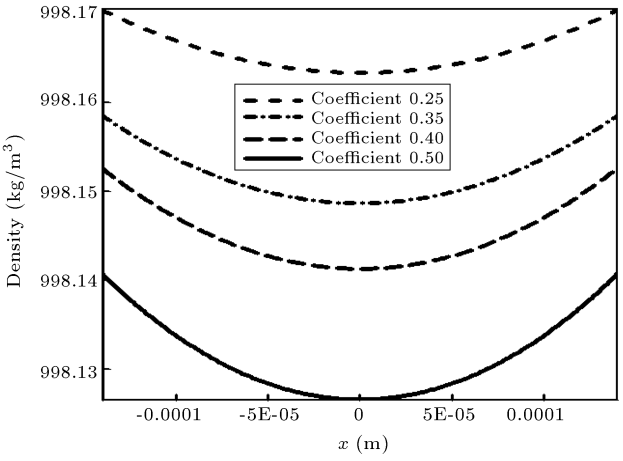

Figure 14. Density changes along with central line.

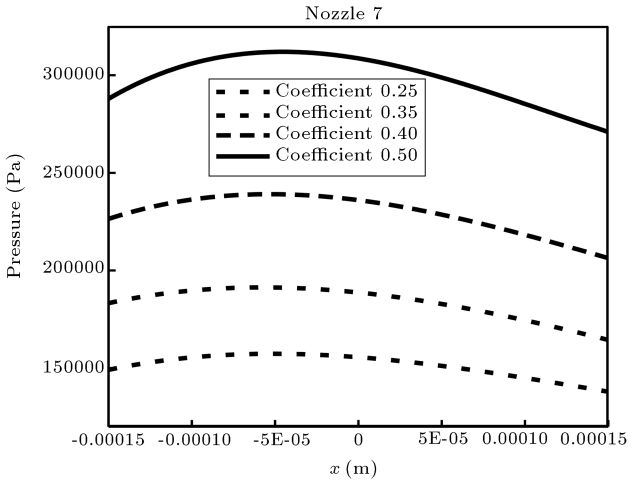

Figure 16. Pressure change graphs for different thermal coefficients and constant 7 nozzle at 50 μs.

creates a unidirectional flow. The maximum pressure occurs in a location near the center of expansion chamber which has the highest temperature. The hottest point has the highest expansion rate and, subsequently, the maximum pressure.

Increase in nozzle diameter significantly decreases the pressure in the expansion chamber because with increase in nozzle diameter, the speed of droplet generation increases, which leads to pressure drop in the expansion chamber.

Figure 16 shows the effects of temperature variations on pressure distribution in the expansion cham-

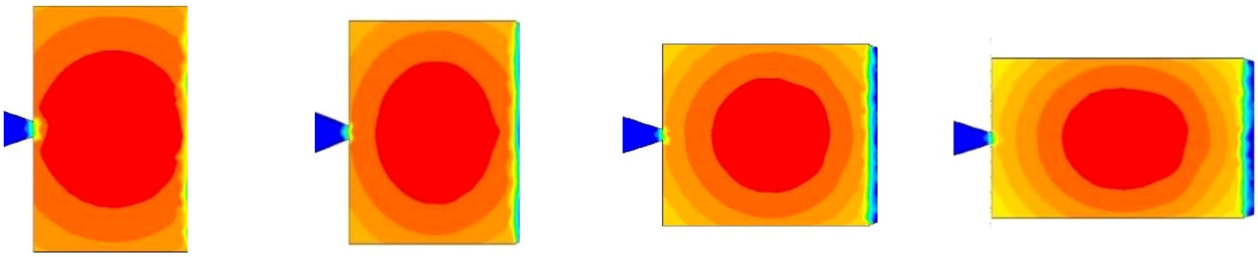

Figure 17. Temperature contour plot for different expansion chamber lengths, from left to right, 300, 250, 200, and 150 micrometers.

ber. With increase in temperature, pressure also increases. Increase in temperature leads to decrease in fluid density and increase its volume. This increase in volume leads to increase in the pressure inside the chamber and fluid tends to compensate for this increase in pressure, which leads to droplet generation. Then, due to the oscillating nature of temperature, the water temperature drops below 283 K. This decrease in temperature leads to decrease in fluid volume, which causes suction at the entrance. This process remains continuous during the operation. Larger temperature changes lead to a greater increase and decrease in fluid volume, which can be clearly seen in pressure graphs. Increase in thermal coefficient leads to significant changes in pressure, leading to different droplet diameters. As can be seen in pressure graphs, increase in temperature leads to increase in pressure inside expansion chamber. This means that increase in temperature increases the volume of the fluid inside the tank, which causes increase in pressure.

Figure 17 shows the temperature contour map inside the expansion chamber. Since the wavelength, λ, and the wavelength bandwidth, b, of the heat wave are constant, the number of peak points on the temperature contour map increases upon increasing the chamber length.

Figure 18 shows the effects of changes in the length of the expansion chamber on the maximum pressure. As can be seen, increase in expansion chamber length increases the maximum pressure. This is due to the fact that the volume of the expansion chamber increases with increase in the length. This means that a larger volume of fluid is affected in expansions and contractions during temperature variations, thus leading to higher pressure inside the tank.

Table 2 shows the effects of change in the expansion chamber length on droplet formation time and droplet diameter for $C = 0.5$. As mentioned before, increase in the length of the expansion chamber leads to increase in pressure, which increases droplet formation. However, droplet generation time is reduced with increase in the length of the expansion chamber because increase in the length also increases the number of waves in the expansion chamber.

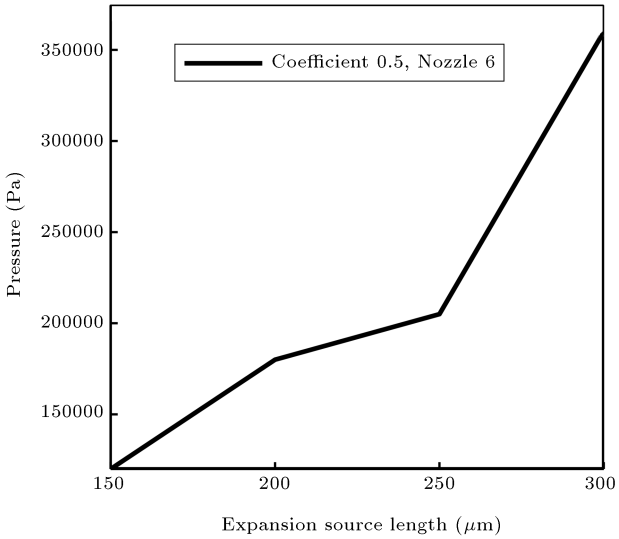

Figure 18. The effects of changes in expansion chamber length on pressure at 50 μs.

Table 2. The effects of changes in tank length on droplet diameter.

Droplet generation time (μs)	Droplet diameter (μm)	Tank length (μm)
23.6	5.9	300
24.22	4.96	250
24.8	3.36	200
25.6	2.67	150

Table 3 shows the effect of changes in temperature and nozzle diameter on droplet diameter and droplet formation time. The effect of nozzle diameter on droplet size is also shown in Figure 19 for thermal coefficient $C = 0.5$. It is obvious that larger nozzles generate larger droplets. On the other hand, increase in thermal coefficient, C, increases droplet diameter. The droplet size is directly related to the viscosity and inversely related to interfacial tension. Both viscosity and interfacial tension decrease with increasingtemperature, but the decrease in viscosity is more severe. Therefore, increasing the temperature causes the droplets to become larger [24].

Table 3. The effect of temperature and nozzle diameter variations on droplet diameter and generation time.

Droplet formation time (μs)	Droplet diameter (μm)	Nozzle diameter (μm)	Thermal coefficient
23.6	5.7	6	0.5
24.2	6.1	7	0.5
25	6.3	8	0.5
21	5	6	0.4
21.8	5.2	7	0.4
22.2	5.3	8	0.4
32.5	4.2	6	0.35
33.5	4.35	7	0.35
35	4.7	8	0.35
59.5	2.5	6	0.25
61.5	2.65	7	0.25
62.8	2.75	8	0.25

According to the results, Droplet formation time is directly proportional to droplet diameter because with increase in droplet size, a longer time duration is required for droplet generation. A sharp increase in formation time is observed for $C = 0.25$. The reason is that despite the formation of droplets in one operational cycle, due to the small size, droplets are swallowed again into the nozzle and released in the second cycle with a larger volume.

It can be concluded from Tables 2 and 3 that the size of the droplets produced by the presented micro pump not only depends on the working fluid properties and the pump geometry, but also is a function of the light beam characteristics such as thermal coefficient, while for the passive droplet generators, the size of the droplets is only a function of the properties of the fluids and the channel geometries [13]. This means that despite the passive droplet generators, the presented micro pump is a controllable droplet generator. Furthermore, the minimum droplet size produced by the passive droplet generators is 10 μm [24], while the droplet size for the current micro pump is lower.

6. Conclusion

In this study, a novel micro pump including an expansion chamber and two rectifier nozzles was proposed that could produce continuous droplets through intermittent heating and cooling of the working fluid. The results demonstrated the good ability of the proposed micro pump for rapid generation of continuous micro droplets. Increase in nozzle diameter led to larger pressure drop in the expansion chamber because of the higher speed of droplet generation. On the other hand, increase in thermal wave amplitude raised the pressure in the expansion chamber, hence larger droplet diameters at the exit of the micro pump. Furthermore, increase in the length of expansion chamber leads to greater pressure, which increased droplet diameter while decreasing droplet generation time.

Nomenclature

b	Wavelength bandwidth
C	Thermal wave amplitude
c_p	Specific heat capacity
F_s	Surface forces
k	Thermal conductivity
p	Pressure
r, r_0	Free variables
Re	Reynolds number
t	Time
T	Temperature
v	velocity

Greek symbols

α_T	Volumetric thermal expansion coefficient
α	Volume fraction function
δ_{kl}	Kronecker delta
$\delta_{\text{th.}}$	Thermal penetration length
η_T	Thermal viscosity coefficient
κ	Interface curvature

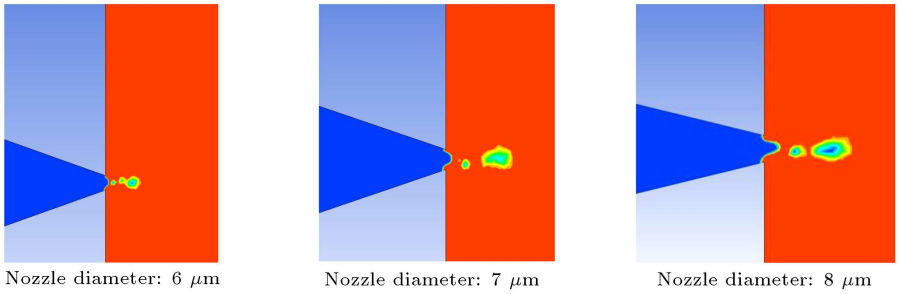

Figure 19. The effect of nozzle diameter on droplet size.

λ	Thermal wave length
μ	Viscosity
σ	Tension
ρ	Density
χ	Free function
δ	Partial derivative symbol
∇	Partial derivative operator

Subscripts

0	Reference state
$\rightarrow$	Vector
th.	Thermal
l	Liquid
g	Gas

References

1. Huang, J., Segura L.J., Wang T., et al. "Unsupervised learning for the droplet evolution prediction and process dynamics understanding in inkjet printing", *Additive Manufacturing*, **35**, p. 101197 (2020).
2. Cech, J., Schrott, W., Slouka, Z., et al. "Enzyme hydrolysis of soybean oil in a slug flow microsystem", *Biochemical Engineering Journal*, **67**, pp. 194–202 (2012).
3. Kaminski, T.S., Scheler, O., and Garstecki, P. "Droplet microfluidics for microbiology: Techniques, applications and challenges", *Lab Chip*, **16**, pp. 2168–2187 (2016).
4. Papadimitriou, V.A., Kruit, S.A., Segerink, L.I., et al. "Droplet encapsulation of electrokinetically-focused analytes without loss of resolution", *Lab Chip*, **20**, pp. 2209–2217 (2020).
5. Barzegar Gerdroodbary, M., Ganji, D.D., Moradi, R., et al. "Application of Knudsen thermal force for detection of CO_2 in low-pressure micro gas sensor", *Fluid Dynamics*, **53**, pp. 812–823 (2018).
6. Mozaffari, M., D'Orazio, A., Karimipour, A., et al. "Lattice Boltzmann method to simulate convection heat transfer in a microchannel under heat flux: Gravity and inclination angle on slip-velocity", *Int. J. Numerical Methods for Heat &Fluid Flow*, **30**(6), pp. 3371–3398 (2020).
7. Dmitry, S.G. and Gatapova, E.Y. "Friction reduction by inlet temperature variation in microchannel flow", *Physics of Fluids*, **33**, p. 062003 (2021).
8. Wang, F., Wang, Y., Bao, W., et al. "Controlling ejection state of a pneumatic micro-droplet generator through machine vision methods", *Int. J. Precis. Eng. Manuf.*, **21**, pp. 633–640 (2020).
9. He, Z., Wang, J., Fike, B.J., et al. "A portable droplet generation system for ultra-wide dynamic range digital PCR based on a vibrating sharp-tip capillary", *Biosensors and Bioelectronics*, **191**, p. 113458 (2021).
10. Rayleigh, J.W.S. "On the instability of jets", *Proc. Lond Math. Soc.*, **10**, pp. 4–13 (1878).
11. Kalantarifard, A., Alizadeh-Haghighi, E., Elbuken, C., et al. "Theoretical and experimental limits of monodisperse droplet generation", *Chemical Engineering Science*, **229**, 116093 (2021).
12. Hoseinpour, B. and Sarreshtehdari, A. "Lattice Boltzmann simulation of droplets manipulation generated in lab-on-chip (LOC) microfluidic T-junction", *J. Molecular Liquids*, **297**, p. 111736 (2020).
13. Teo, A.J.T., Yan, M., Dong, J., et al. "Controllable droplet generation at a microfluidic T-junction using AC electric field", *Microfluidics and Nanofluidics*, **24**(3), pp. 1–9 (2020).
14. Tan, Y.C., Cristini, V., and Lee, A.P. "Monodispersed microfluidic droplet generation by shear focusing microfluidic device", *Sensors and Actuators B: Chemical*, **114**(1), pp. 350–356 (2006).
15. Besanjideh, M., Shamloo, A., and Kazemzadeh Hannani, S. "Enhanced oil-in-water droplet generation in a T-junction microchannel using water-based nanofluids with shear-thinning behavior: A numerical study", *Physics of Fluids*, **33**, p. 012007 (2021).
16. Bao, W., Wang, Y., Yang, B., et al. "Some considerations for designing a pneumatic micro-droplet generator", *J. Micromech. Microeng.*, **31**, p. 045008 (2021).
17. Wang, F., Wang, Y., Bao, W., et al. "Controlling ejection state of a pneumatic micro-droplet generator through machine vision methods", *Int. J. Precis. Eng. Manuf.*, **21**, pp. 633–640 (2020).
18. Guo, Q., Su, X., Zhang, X., et al. "A review on acoustic droplet ejection technology and system", *Soft Matter*, **17**, pp. 3010–3021 (2021).
19. Li, H., Liu, J., Liu, Y., et al. "Development of a resonant piezoelectric micro-jet for high-viscosity liquid using a longitudinal transducer", *Mechanical Systems and Signal Processing*, **146**, p. 107012 (2021).
20. Xuan, L.P., Quang, L.D., Quoc, T.V., et al. "Development of a microfluidic flow-focusing droplet generating device utilising rapid prototyping technique", *Int. J. Nanotechnology*, **17**, pp. 708–721 (2020).
21. Madou, M., Zoval, J., Jia, G., et al. "Lab on a CD", *Annu. Rev. Biomed. Eng.*, **8**, pp. 601–628 (2006).
22. Saint Vincent, M.R., Chraïbi, H., and Delville, J.P. "Optical flow focusing: Light-induced destabilization of stable liquid threads", *Phys. Rev. Appl.*, **4**, p. 044005 (2015).
23. Kazuno, N., Tsukahara, T., and Motosuke, M. "Laplace pressure versus Marangoni convection in photothermal manipulation of micro droplet", *Eur. Phys. J. Special Topics*, **226**, pp. 1337–1348 (2017).
24. Zhu, P. and Wang, L. "Passive and active droplet generation with microfluidics: a review", *Lab Chip*, **17**, pp. 34–75 (2017).

25. Çetin, B., Bülent Özer, M., and Ertuğrul Solmaz, M., et al. "Microfluidic bio-particle manipulation for biotechnology", *Biochemical Engineering Journal*, **92**, pp. 63–82 (2014).

26. Yariv, E. and Brenner, H. "Flow animation by unsteady temperature fields", *Physics of Fluids*, **16**(11), p. L95 (2004).

27. Pal, D. and Chakraborty, S. "Axial flow in a two-dimensional microchannel induced by a travelling temperature wave imposed at the bottom wall", *J. Fluid Mech.*, **848**, pp. 1040–1072 (2018).

28. Pal, D. and Chakraborty, S. "Fluid flow induced by periodic temperature oscillation over a flat plate", *Physics of Fluids*, **27**(5), p. 053601 (2015).

29. Weinert, F.M., Kraus, J.A., Franosch, T., et al. "Microscale fluid flow induced by thermoviscous expansion along a traveling wave", *Physical Review Letters*, **100**(16), p. 164501 (2008).

30. Weinert, F.M., Wühr, M., and Braun, D. "Light driven microflow in ice", *Applied Physics Letters*, **94**(11), p. 113901 (2009).

31. Weinert, F.M. and Braun, D. "Optically driven fluid flow along arbitrary microscale patterns using thermoviscous expansion", *J. Applied Physics*, **104**(10), p. 104701 (2008).

32. Cui, W., Yesiloz, G., and Ren, C.L. "Numerical analysis on droplet mixing induced by microwave heating: Decoupling of influencing physical properties", *Chemical Engineering Science*, **224**, p. 115791 (2020).

33. Xia, Z., Zhao, Y., Yang, Z., et al. "The simulation of droplet impact on the super-hydrophobic surface with micro-pillar arrays fabricated by laser irradiation and silanization processes", *Colloids and Surfaces A: Physicochemical and Engineering Aspects*, **612**, p. 125966 (2021).

34. Zhu, L., Monteil, D.T., Wang, Y., et al. "Fluid dynamics of flow fields in a disposable 600-mL orbitally shaken bioreactor", *Biochemical Engineering Journal*, **129**, pp. 84–95 (2018).

35. Guan, H., Wang, J., Wei, Z., et al. "Numerical analysis of the interaction of 3D compressible bubble clusters", *Appl. Math. Mech.-Engl. Ed.*, **40**, pp. 1181–1196 (2019).

Biographies

Mohammad Mehrabi received his BSc degree in 2015 from Majlesi branch of Islamic Azad University and his MSc degrees in 2018 from Najafabad branch of Islamic Azad University. Both BSc and MSc degrees are in the field of Mechanical Engineering. His research interests are two phase flows in micro/nano fluidics and droplet generation.

Amir Homayoon Meghdadi Estefani is an Associate Professor in the Faculty of Engineering, Najafabad branch, Islamic Azad University. He received his PhD in Nanotechnology Engineering from the University of Tehran and a BSc in Mechanical Engineering, Energy Conversion from the University of Isfahan Technology. His current research focuses on fluid mechanics, thermodynamics, nano fluids, and micro/nano fluidics.